Journal of Nuclear Materials 390–391 (2009) 768–772

Contents lists available at ScienceDirect

Journal of Nuclear Materials

journal homepage: www.elsevier.com/locate/jnucmat

Effect of external perturbation fields on divertor particle and heat loads during ELMs at JET

S. Jachmich [a,*], Y. Liang [b], G. Arnoux [c], T. Eich [d], W. Fundamenski [c], H.R. Koslowski [b], R.A. Pitts [e], JET-EFDA Contributors [1]

[a] Laboratory for Plasma Physics, Ecole Royale Militaire/Koninklijke Militaire School, EURATOM-Association 'Belgian State', Av. de la Renaissance 30, B-1000 Brussels, Partner in the Trilateral Euregio Cluster (TEC), Belgium
[b] Institut fuer Plasmaphysik, Euratom Association, D-52425 Juelich, Partner in the Trilateral Euregio Cluster (TEC), Germany
[c] EURATOM-UKAEA Fusion Association, Culham Science Centre, United Kingdom
[d] Max-Planck Institut fuer Plasmaphysik, Euratom Association, Garching, Germany
[e] Centre de Recherches en Physique des Plasmas, Association EURATOM, Conférédation Suisse, EPFL, 1015 Lausanne, Switzerland

ARTICLE INFO

PACS:
52.55.Rk
52.40.Hf
52.70.−m
28.52.−s

ABSTRACT

Peak heat fluxes arriving at the JET-divertor during Type-I ELMs have been successfully reduced by applying externally magnetic perturbation fields. The ELM-frequency in these plasmas strongly increases, leading to smaller ELM-size. The concomitant density losses, known as pump-out effect, have been recovered using inboard divertor gas fuelling, albeit with a degradation of the energy confinement. Langmuir probe analysis has shown that the magnetic perturbation drastically reduces the ELM-peak heat flux mostly via a reduction in particle flux, but at the price of higher inter-ELM fluxes.

1. Introduction

The heat loads during Type-I ELMs are a major concern for the ITER-divertor and must be drastically reduced from their predicted natural levels if material damage limits are not to be exceeded [1,2]. Amongst several techniques currently being investigated for ELM mitigation, ergodization of the plasma edge using an externally applied magnetic perturbation field is a very promising avenue [3]. At JET this technique has been tested in a variety of plasma shapes at low and high triangularity by operating the error field correction coils (EFCC) in an $n = 1$ or $n = 2$ configuration [4,5]. Particle and heat fluxes to the plasma-facing components have been measured by Langmuir probes embedded in the new MkIIHD-divertor and in the outer wall guard limiters.

The JET error field correction coil system consists of four magnetic perturbation coils mounted at equally spaced toroidal locations. The EFCC can be operated either in an $n = 1$ configuration, which leads to a strong core perturbation and can seed locked modes or in an $n = 2$ configuration, which provides good edge ergodization. Due to the present limitation of the available coil current for the $n = 2$ configuration experiments thus far have been performed mostly in the $n = 1$ configuration from which all data presented here are obtained.

The experiments have been carried out in low and high triangularity (δ) discharges with δ ranging from 0.29 to 0.45 and with the outer strike point placed in the middle of the new load-bearing septum replacement tile (LBSRP) [6], which allows high triangularity operation with high input power. It is worth mentioning that the choice of the strike point location, which leads to poorer divertor pumping and hence higher natural ELM-frequency, was based on diagnostic needs. Fig. 1 shows the time evolution of several important parameters for a typical high triangularity discharge (JPN #69555), in which the EFCC are applied. During the flat top of this Type-I ELMy H-mode discharge ($I_p = 1.8$ MA, $B_t = 2.16$ T, $q_{95} = 4.4$, $P_{NBI} = 9.5$ MW, $P_{RF} = 1.0$ MW, $\langle n_e \rangle = 5 \times 10^{19}$ m^{-3}), the EFCC are energised with currents of 2 kA $\times$ 16 turns. At these plasma currents and input power, natural ELMs appear at a frequency $f_{ELM} \sim 30$ Hz and release $\Delta W_{ELM} \approx 130$ kJ of the pedestal energy. During the EFCC-phase the ELM-frequency strongly increases to about 90 Hz with ΔW_{ELM} dropping to values which lie within the noise level of the diamagnetic energy signal. A power-scan has revealed the ELMs remain Type-I despite their higher frequency and lower amplitude. The loss of core and edge density during the error field application, often referred to as the pump-out effect, is not seen as increased particle flux, as indicated by the ion saturation current, at the divertor in the inter-ELM phases (Fig. 1). At the ELM-peak, the particle flux and heat flux are strongly reduced dur-

* Corresponding author.
E-mail address: s.jachmich@fz-juelich.de (S. Jachmich).

[1] See appendix of M. Watkins et al., Fusion Energy 2006 (Proc. 21st Int. Conf. Chengdu) IAEA, Vienna (2006).

0022-3115/$ - see front matter © 2009 Elsevier B.V. All rights reserved.
doi:10.1016/j.jnucmat.2009.01.204

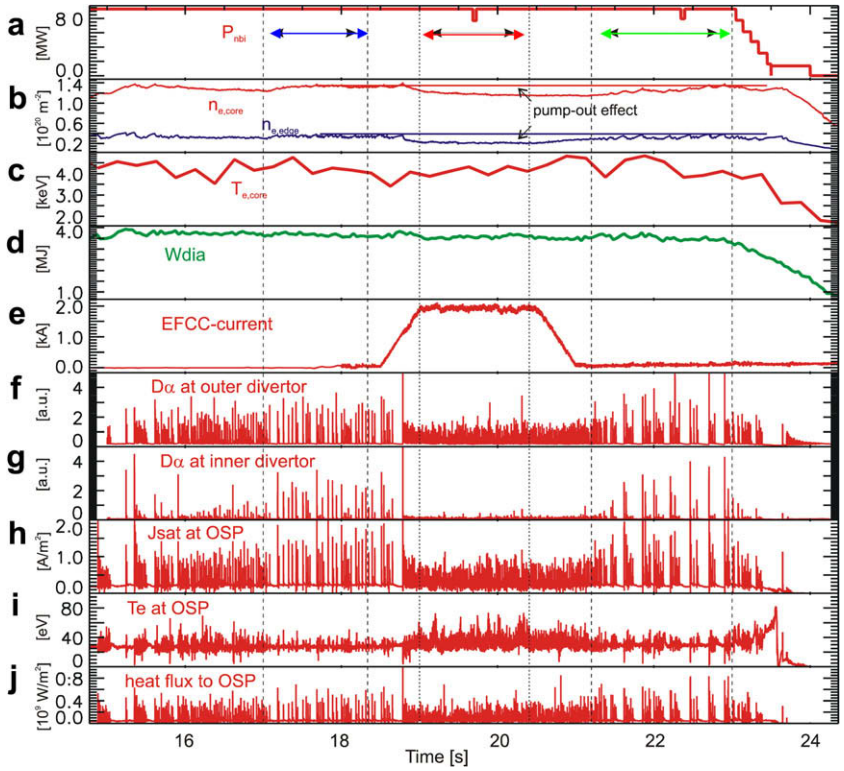

Fig. 1. Overview of high-δ ELMy H-mode discharge, showing (a) input power, (b) core and edge density, (c) core temperature, (d) diamagnetic energy, (e) EFCC-current, (f) D_α-recycling at outer divertor, (g) D_α-recycling at inner divertor, (h) particle flux, (i) electron temperature and (j) heat flux at outer divertor strike point (OSP).

ing the EFCC-phase (Fig. 1(h) and (j)), since less particles are lost during the ELMs. This is confirmed by the decrease of the density drop in the edge interferometer channel during the ELM (from 2.8×10^{18} m^{-2} to 1.4×10^{18} m^{-2}). The confinement is almost preserved due to a strong increase of the electron and ion temperatures. Since the EFCC induce an offset in the diamagnetic energy measurement due to magnetic pick-up, the plasma energy must be inferred from other diagnostics. Assuming that the energy partition between electrons and ions remains unchanged, the electron thermal energy content in the plasma can serve as a measure of the confinement. Despite the observation that 30% of particles are lost, the thermal electron energy drops only by 8%.

2. Divertor target profiles

The LBSRP in the JET-divertor is equipped at 12 poloidal locations with a total of 27 Langmuir probes, of which seven can be operated as triple probes with a maximum temporal resolution of 100 μs. Target profiles during the ELMs have been obtained by coherently averaging the detected ELM-peaks. Fig. 2 shows the result for the particle flux J_{sat}, electron temperature T_e and heat flux Q_p for three phases in the discharge, as indicated by the arrows in Fig. 1. The heat flux is estimated from J_{sat} and T_e assuming a sheath transmission factor of $\gamma = 8$. One should note that the profiles in Fig. 2(c) reflect the heat flux peak values, which is not necessarily the product of the J_{sat}- and T_e-peak profiles, since the saturation current and electron temperature reach their maximum at different times during the ELM [7]. As reported earlier [8], the flux profiles tend to broaden during the ELMs. The EFCC do not cause additional broadening or shift of the profile, but the ELM-peaks are drastically reduced over the whole profile by about 40%. There is only a small effect on T_e during both the ELM and inter-ELM phases. It is very much worthwhile mentioning that the interaction of the ELMs with the outer wall is also diminished as observed by the outer wall guard limiter probes as it will be shown below.

Since the EFCC create a toroidally asymmetric perturbation, the fluxes might not be toroidally uniform. To study this, a phase scan has been performed, where the polarity of coil currents is changed such that the resulting perturbation is shifted toroidally by 90°. For operational reasons, only three phases have been tested. The observation that in all three phases the particle and heat fluxes during the ELM are reduced by the EFCC demonstrates that the ELM-mitigation is not a local effect. Using plasma with large outer and inner wall clearances it has been shown that interactions with the outer wall are not enhanced during the EFCC-phase. In addition, a large drop in the divertor fluxes has also been observed in these high clearance discharges.

The ELMs amplitude is known to have a distribution function of finite width, some ELMs being larger than others for given plasma conditions. All ELM-mitigation techniques must therefore not only demonstrate that the ELM-peak amplitudes are reduced on average but that the probability distribution of the peak amplitude is also not broadened. As shown in Fig. 3, the histograms of ELM-peaks measured by probes at the outer strike point location and at the outboard limiter are clearly shifted towards smaller heat and particle fluxes.

3. Compensation of the density pump-out effect

As pointed out earlier, plasmas with external magnetic field perturbation suffer from strong density pump-out. In order to compensate for this, gas fuelling has been applied during the main heating phase from the inboard side of the divertor. A series of low-triangularity discharges with different gas fuelling levels has been performed. Data averaging has been done for 500 ms

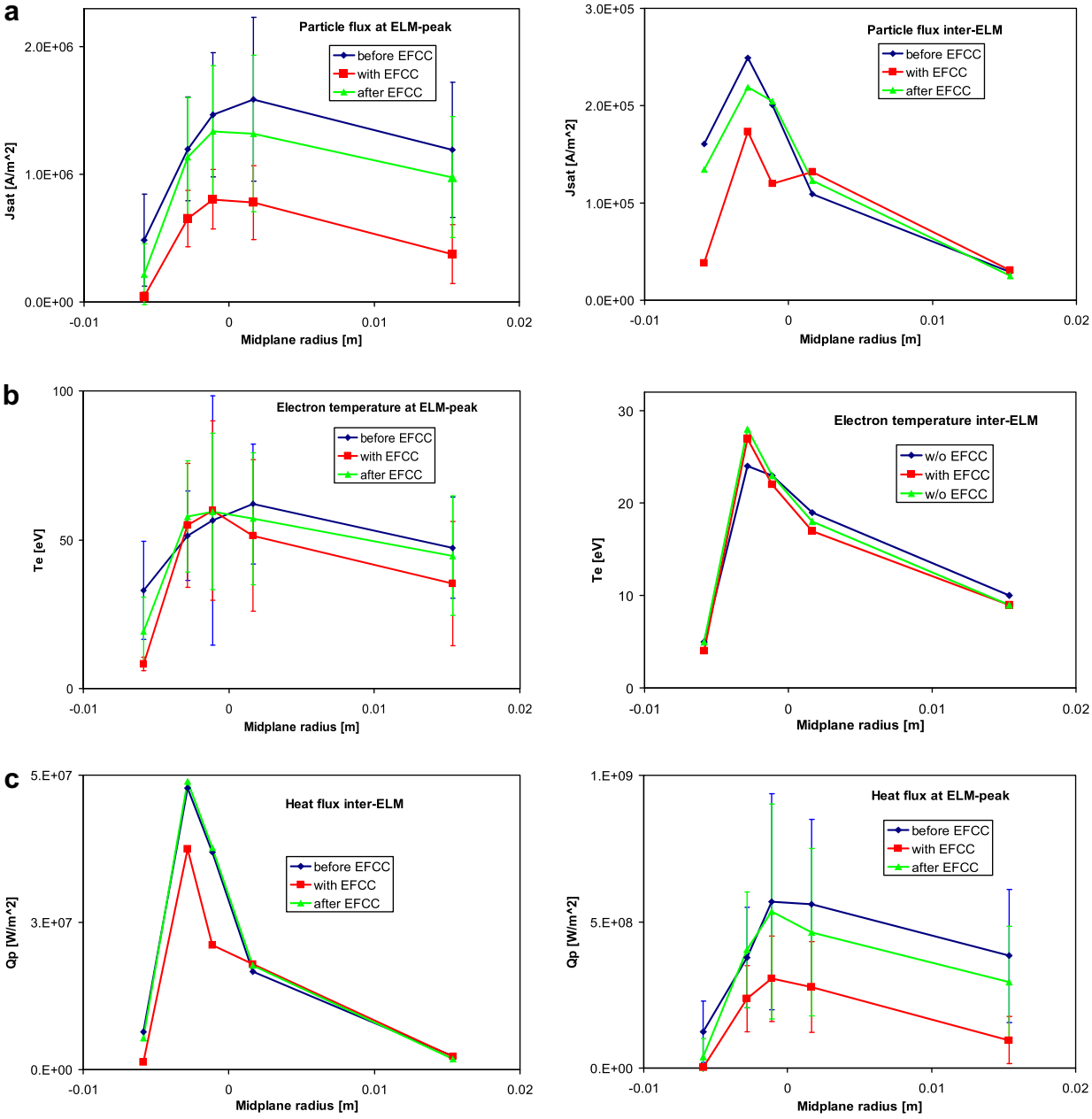

Fig. 2. Divertor target profiles for high-δ discharge of ELM-peaks and inter-ELM. The data have been averaged for the time windows indicated by the arrows in Fig. 1.

at the end of the EFCC flat top phase and during an appropriate time window following the EFCC switch-off. Fig. 4 illustrates that already modest gas puffing levels (5×10^{21} elec/s) are sufficient to compensate the lost density during the EFCC phase of an unfuelled reference discharge. As expected, the ELM-frequency increases slightly with higher fuelling rates in addition to the increase caused by the magnetic perturbation. The loss of density leads to a degradation of the confinement as shown in Fig. 5, where the energy confinement time is normalised to the ITER-H98(y,2)-scaling. With stronger fuelling the density can be recovered, but the confinement decreases further since the increase in core and edge temperature is insufficient to compensate for the lost thermal energy. In this experimental series only plasma densities up to 80% of the Greenwald density were achieved.

Unlike in the high-δ discharges, during EFCC phases at lower δ, the inter-ELM particle and heat fluxes are increased, typically by about 50% in an unfuelled discharge. The EFCCs have no beneficial effect on the inter-ELM losses, but they redistribute the energy losses carried by the ELMs with respect to inter-ELM phases. To estimate the energy per ELM arriving at the target, the individual probe signals have been integrated in time. After subtracting the inter-ELM losses and weighting the remaining energy by the ELM-number, the averaged energy per ELM arriving at the outer target is obtained:

$$W_{\mathrm{ELM,target}} = 2\pi\left[\int\int_{t_1}^{t_2} Q_{\mathrm{p}}(t,R)dt\,R\sin\theta_{\perp}(R)dR/(t_2-t_1) - \int Q_{\mathrm{p,inter}}(R)R\sin\theta_{\perp}(R)dR\right]\Big/ f_{\mathrm{ELM}} \quad (1)$$

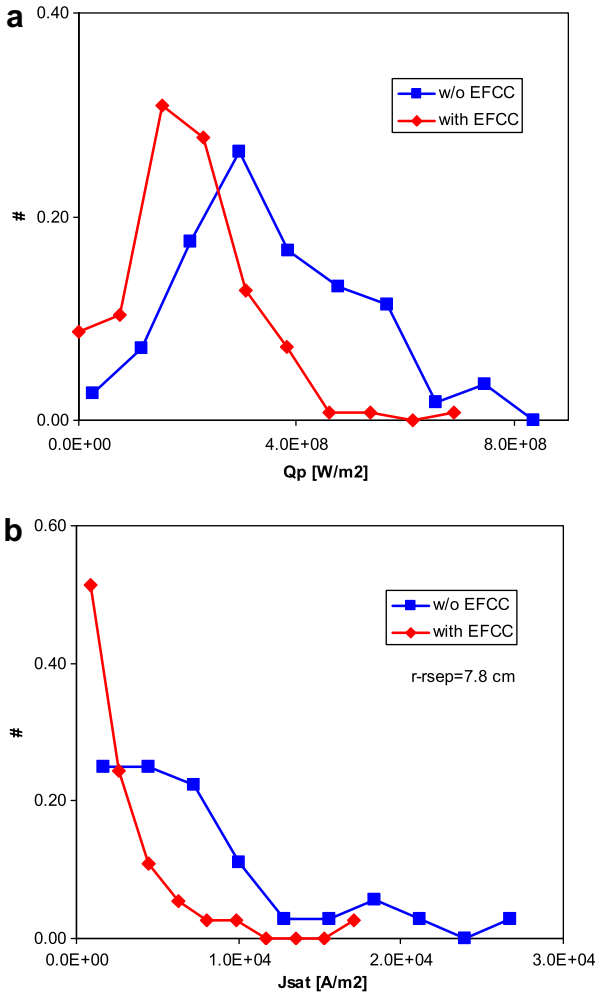

Fig. 3. ELM-peak histogram normalised to the total number of ELMs (a) of heat flux at outer divertor target and (b) of particle flux at outboard limiter.

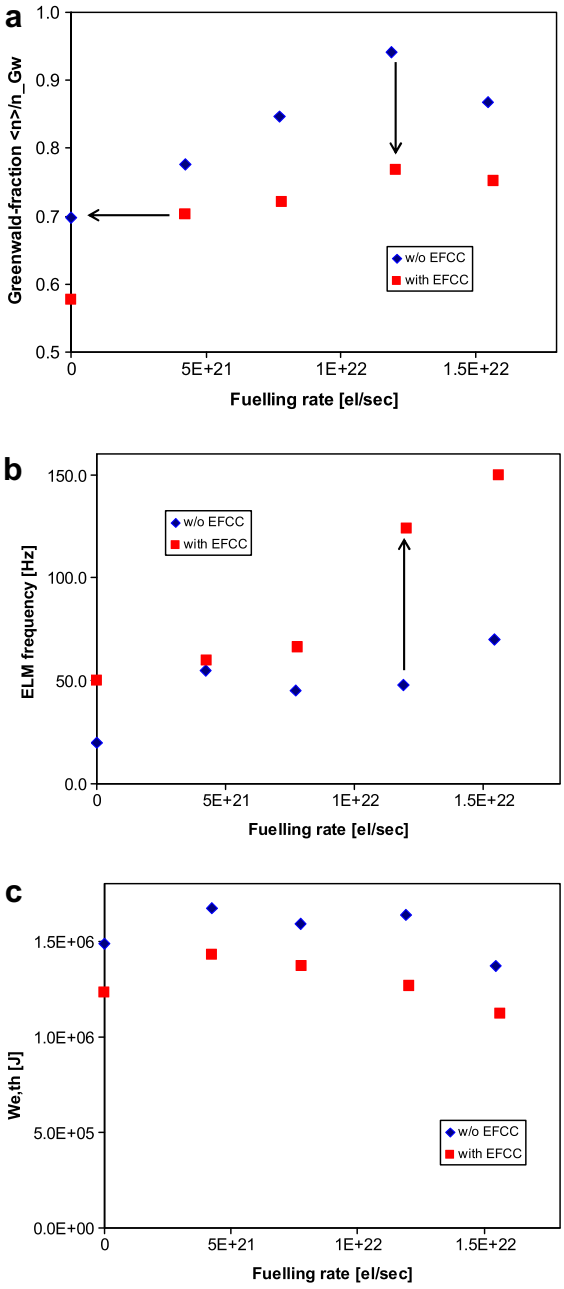

Fig. 4. Greenwald density fraction, ELM-frequency and thermal electron energy content plotted against increasing fuelling rate.

>with Q_p the parallel heat flux measured by a Langmuir probe at major radius R, $\theta_\perp$ the angle between the field line and its perpendicular projection onto the divertor plate, $Q_{p,inter}$ the parallel inter-ELM heat flux and t_1 and t_2 times in the discharge specifying a window over which the data have been integrated. Table 1 summarizes the results. Note first that the ratios of ELM-peak to inter-ELM losses are strongly reduced during the EFCC-phase (from ~50 down to ~17). The comparable reduction of the particle flux and heat flux ELM-peaks suggests that the magnetic perturbation is mainly affecting the convective transport channel. In contrast, the inter-ELM fluxes are increased by the EFCC. In the unfuelled, low-δ discharge about 243 kJ were lost per ELM without the EFCC, which decreases to 91 kJ with the EFCCs on. Assuming a fractional radiative energy loss of 25% of the ELM-energy [9], one expects 182 kJ (without EFCC) and 68 kJ (with EFCC) arriving at the inner and outer divertor targets. Accounting the measured ELM-energy at the outer target (cf. Table 1) and assuming the remaining energy to be completely deposited at the inner target, we find ratios for the inner/outer-asymmetry in the range from 1.4 to 1.7, which is in fair agreement with IR-observations where asymmetries by about 2:1 have been found on JET [10].

4. Conclusions

External magnetic perturbation field experiments have been shown to mitigate the ELM-peaks arriving at the outer target solely by reducing the particle losses during the ELM. The electron temperature at the target remains high, but does not seem to increase. In low triangularity plasmas the inter-ELM fluxes are increased, together with a loss of electron energy and degradation of confinement. The density pump-out can be recovered by gas fuelling, but at the expense of a further degradation in the energy confinement. Furthermore, even with intense gas puffing only target densities up to a Greenwald fraction of 80% can be reached in low-δ

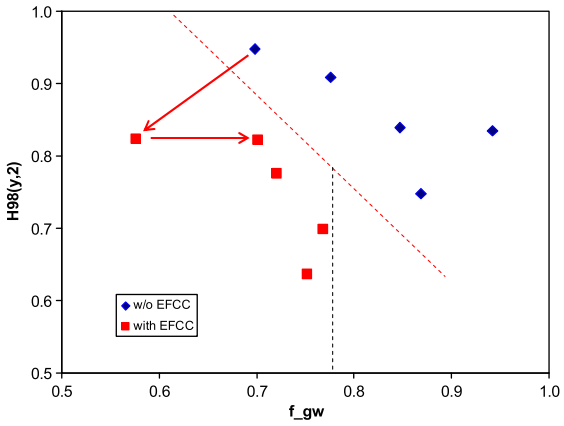

Fig. 5. Confinement factor versus Greenwald density fraction for discharge phase without EFCC (rhombs) and with EFCCs (squares). The arrows indicate the change in confinement, when the EFCCs are applied and when the discharge is refuelled.

Table 1
Outer divertor target fluxes derived from probes.

	Particle flux		Heat flux	
	w/o EFCC	With EFCC	w/o EFCC	With EFCC
Inter-ELM	4.6 [10^{22}/s]	6.9 [10^{22}/s]	1.3 [MW]	2.2 [MW]
ELM-peak	1.4 [10^{24}/s]	0.86 [10^{24}/s]	79 [MW]	43 [MW]
Total flux	1.0 [10^{23}/s]	1.2 [10^{23}/s]	2.9 [MW]	3.4 [MW]
Loss per ELM	2.7 [10^{21}]	0.93 [10^{21}]	77 [kJ]	25 [kJ]
f_{ELM}			21 [Hz]	50 [Hz]
ΔW_{dia}			243 [kJ]	91 [kJ]
In/out ratio			1.4	1.7

plasmas. The density pump-out makes divertor conditions more difficult for detachment achievement and increases the inter-ELM heat fluxes. ELM-mitigation by magnetic perturbations is a viable and attractive technique, but some reduction of confinement must be accepted.

Acknowledgements

This work, supported by the European Communities under the contract of Association between EURATOM/Belgian State, was carried out within the framework of the European Fusion Development Agreement. The views and opinions expressed herein do not necessarily reflect those of the European Commission.

References

[1] D.J. Campbell, Phys. Plasmas 8 (2001) 2041.
[2] G. Federici, Plasma Phys. Control. Fus. 45 (2003) 1523.
[3] T. Evans et al., Nat. Phys. 2 (2006) 419.
[4] Y. Liang et al., Phys. Rev. Lett. 98 (2007) 265004.
[5] Y. Liang et al., Plasma Phys. Control. Fus. 49 (2007) B581.
[6] T. Todd et al., in: SOFT-23rd Symposium on Fusion Technology, Venice, Italy, 2004.
[7] S. Jachmich et al., in: Proceedings of the 28th EPS Conference on Controlled Fusion and Plasma Physics, 25A, 2001, 1625.
[8] S. Jachmich et al., J. Nucl. Mater. 363–365 (2007) 1050.
[9] R. Pitts et al., Nucl. Fus. 47 (2007) 1437.
[10] Th. Eich et al., Plasma Phys. Control. Fus. 49 (2005) 573.